Available online at www.sciencedirect.com
SCIENCE DIRECT®
ELSEVIER
Deep-Sea Research I 52 (2005) 1461–1476
DEEP-SEA RESEARCH PART I
www.elsevier.com/locate/dsr

Reassessing the dissolution of marine carbonates: II. Reaction kinetics

M. Gehlen[a,*], F.C. Bassinot[b], L. Chou[c], D. McCorkle[d]

[a]*Laboratoire des Sciences du Climat et de l'Environnement (LSCE), UMR CEA-CNRS, Bât.701, Orme des Merisiers, CEA/Saclay, 91191 Gif-sur-Yvette Cedex, France*
[b]*Laboratoire des Sciences du Climat et de l'Environnement (LSCE), UMR CEA-CNRS, Bât. 12, avenue de la Terrasse, 91198 Gif-sur-Yvette Cedex, France*
[c]*Laboratoire d'Océanographie Chimique et Géochimie des Eaux, Campus de la Plaine, CP 208, 2 Boulevard du Triomphe, Université Libre de Bruxelles, 1050 Brussels, Belgium*
[d]*Woods Hole Oceanographic Institution (WHOI), Department of Geology & Geophysics, 100 C McLean Lab, Woods Hole, MA 02543, USA*

Received 26 July 2004; received in revised form 7 January 2005; accepted 9 March 2005
Available online 2 June 2005

Abstract

We studied dissolution kinetics of the carbonate fraction $>150\,\mu m$ of sediments sampled along two bathymetric transects in the eastern tropical Atlantic: the Sierra Leone Rise (SLR) and the Cape Verde Plateau (CVP). The reaction was followed by monitoring solution pH during freedrift experiments lasting between 46 and 50 h (20 °C, $pCO_2 \approx 3100$ ppm and 1 atm pressure). The alkalinity reached at the end of the dissolution experiments ranged between 2.444 and 2.798 meq/kg_{sw}. The dissolution time series was extrapolated to equilibrium by fitting an empirical relation to the data. The estimated asymptotic concentration products ($[Ca^{2+}]_\infty \times [CO_3^{2-}]_\infty$, for $t \to \infty$ and $dA_c/dt = 0$) range from 4.27×10^{-7} to 6.77×10^{-7} mol^2/kg_{sw}^2. These asymptotic concentration products are comparable with the stoichiometric concentration product of aragonite (6.56×10^{-7} mol^2/kg_{sw}^2) and calcite ($4.37\ (\pm 0.22) \times 10^{-7}$ mol^2/kg_{sw}^2) derived for the same sediment material during long-term equilibration experiments. They are indicative of the presence of trace amounts of a higher solubility carbonate phase in sediments of the shallow stations (SLR station *A*, 2637 m; CVP station *M*, 3104 m). While it is likely that this phase is aragonite, the presence of authigenic carbonate precipitated in contact with supersaturated bottom waters cannot be excluded. Calcite is the main dissolving carbonate mineral in sediments from deeper stations. The order of reaction is always greater than unity. It varies between 1.4 (SLR station C) and 2.8 (CVP station M2), with an average $n = 2.3 \pm 0.4$. The higher order reaction is explained in terms of a multiphase system. Specific rate constants range from 0.09 to 0.53 meq/m^2/d.

Keywords: Marine sediments; Biogenic carbonate; Dissolution kinetics

*Corresponding author. Tel.: +33 1 69088672; fax: +33 1 69087716.
E-mail address: marion.gehlen@cea.fr (M. Gehlen).

0967-0637/$ - see front matter © 2005 Elsevier Ltd. All rights reserved.
doi:10.1016/j.dsr.2005.03.011

1. Introduction

The variability of calcium carbonate ($CaCO_3$) content of marine sediments serves as a proxy for past oceanic productivity and deep-water carbonate chemistry (Berger et al., 1989; Curry and Lohmann, 1985; Lyle et al., 1988). The record of sedimentary $CaCO_3$ displays strong glacial–interglacial cycles (Farrel and Prell, 1989). On these time scales, the sediments participate in the ocean carbon cycle by balancing input fluxes of alkalinity derived from continental weathering through the burial of $CaCO_3$. The mechanism maintains the global ocean alkalinity budget at steady state and feeds back on atmospheric pCO_2 (e.g. Broecker and Takahashi, 1978, Opdyke and Walker, 1992, Archer and Maier-Reimer, 1994; Sigman et al., 1998; Archer et al., 2000) and is likely to contribute to the future neutralization of anthropogenic CO_2 on thousand year time-scales (Archer et al., 1998).

The flux of $CaCO_3$ entering the sediment as the remains of pelagic organisms (coccolithophorids, foraminifera, pteropods) depends upon surface productivity, the saturation state of bottom waters and diagenetic reactions. The saturation state of bottom waters is set by the carbonate ion concentration, together with the pressure (depth of water column) and temperature dependence of carbonate mineral solubility (Broecker and Takahashi, 1978; Mucci, 1983; Millero, 1995). The release of CO_2 to pore waters during aerobic organic matter decay is an additional potentially important driving force for $CaCO_3$ dissolution in surface sediments (e.g. Emerson and Bender, 1981; Archer et al., 1989; Berelson et al., 1990; Hales et al., 1994; Cai et al., 1995; Jahnke et al., 1997; Jahnke and Jahnke, 2004). Carbonate dissolution driven by metabolic CO_2 can result in a substantial alkalinity flux from sediments deposited above the saturation depth and was proposed as a feedback mechanism on atmospheric pCO_2 (Archer and Maier-Reimer, 1994). Our capability to interpret the sedimentary record of $CaCO_3$ in terms of past environmental conditions, as well as to evaluate model forecasts of future changes of the coupled oceanic–atmospheric C cycle, relies in part on the accurate estimation of $CaCO_3$ dissolution kinetics and associated alkalinity fluxes.

Dissolution kinetics of $CaCO_3$ have been extensively studied over the past 30 years (e.g. Morse and Berner, 1972; Ingle et al., 1973; Berner and Morse, 1974; Berner, 1976; Morse, 1978; Honjo and Erez, 1978; Plummer et al., 1978; Keir, 1980; Walter and Morse, 1985; Chou et al., 1989; Van Cappellen et al., 1993; Arakaki and Mucci, 1995; Morse and Arvidson, 2002). Empirical studies of the dissolution behavior of biogenic carbonates in seawater yielded a high order dependence ($n = 4.5$) of the dissolution reaction on the degree of undersaturation of seawater (Keir 1980). These results were challenged by Hales and Emerson (1997b) based upon the reassessment of experimental data Keir (1980) had obtained for synthetic calcite. They concluded that the rate of dissolution is linearly dependent on undersaturation and proposed that the high reaction order reported by Keir (1980) could be ascribed to uncertainties linked to the saturation state of the experimental seawater solution. First-order calcite dissolution kinetics proved to be more consistent with the interpretation of in-situ pore water pH measurements (Hales and Emerson, 1997a, b). A satisfying reproduction of pore water profiles through diffusion–reaction models is, however, not a proof per se of the validity of a kinetic expression (Gehlen et al., 1999).

The use of synthetic calcite, which is a homogeneous phase with a set of well-defined characteristics (e.g. trace element composition, degree of crystallinity, specific surface) makes it possible to resolve individual reactions (Chou et al., 1989; Van Cappellen et al., 1993; Arakaki and Mucci, 1995) and thus has distinct advantages in the context of kinetics studies. However, biogenic carbonates are heterogeneous, and non-homogeneous dissolution has been reported in the past (Broecker et al., 1991; Lohmann, 1995; McCorkle et al., 1995; Martin et al., 2000). Thus there are potential problems with using a synthetic mineral as an analog for a biogenic mineral phase. There is a clear need for kinetic experiments to be carried out with natural marine carbonates.

We addressed this need by studying the dissolution kinetics of core top sediments sampled along two bathymetric transects in the eastern equatorial Atlantic, on the Sierra Leone Rise (SLR) and the Cape Verde Plateau (CVP). The size fraction

greater than 150 μm was used. It consists of foraminifera shells and fragments. There are two reasons for selecting a specific size fraction, rather than working with the bulk sediment. First, the presence of clay minerals within bulk sediments would most likely result in an artifact linked to reactions at clay mineral surfaces. Second, the importance of foraminifera in paleoenvironmental reconstructions makes the understanding of their dissolution behavior an important goal in itself. This paper focuses on the kinetics of marine carbonate dissolution. The solubility is discussed in Part I (Gehlen et al., 2005).

2. Study area

Sediment cores were collected aboard the R.V. *Knorr* (winter 1998) along two bathymetric transects in the eastern equatorial Atlantic (SLR and CVP). Several previous studies discussed the carbonate sediment of this region (Archer et al., 1989; Curry and Lohmann, 1986, 1990; Dubois and Prell, 1988). The geographic locations of sampling sites are listed in Table 1 and shown in Fig. 1.

3. Material

Sediment cores were collected with a multicorer. Cores for which there was evidence of disturbance of the sediment–water interface or turbidity of the overlying water were excluded from processing. Sediments were extruded and core-tops were sliced into 1 cm-thick samples. Complete pteropod shells were observed occasionally in sediments from stations A and B on the SLR transect. No pteropod shells or fragments were identified in samples selected for this study. Sediments were transferred into plastic containers and stored at 2 °C without further conditioning or processing. Core-top sediments were sub-sampled on shore. Sediments were gently wet-sieved in order to separate the >150 μm size fraction. Care was taken to avoid breaking individual carbonate particles. The size fractions were cleaned by repeated sonification to remove fines from inside foraminifera chambers, and rinsed with distilled water before being oven-dried to constant weight.

4. Methods

4.1. Dissolution experiments

The dissolution experiments were carried out in artificial seawater. Seawater was prepared according to Grasshoff et al. (1983), but without adding carbonate alkalinity. During the experiments two batches of artificial seawater were used. Soluble reactive phosphate levels were analyzed following the standard molybdenum-blue colorimetric

Table 1
Location and depth of sampling sites

Stat.	Latitude	Longitude	Depth (m)	TCO_2 (mmol/kg$_{sw}$)	A_t (meq/kg$_{sw}$)	Ω_a	Ω_c	CO_3^{2-} (μmol/kg$_{sw}$)
Sierra Leone Rise								
A	5°07.1N	21°00.5W	2637	2.172	2.336	1.04	1.60	113.4
C	5°31.9N	21°48.4W	3593	2.182	2.338	0.82	1.25	106.7
E	7°00.0N	24°36.8W	4202	2.180	2.344	0.76	1.15	110.2
G	8°57.1N	24°29.0W	4930	2.193	2.350	0.64	0.96	104.9
Cape Verde Plateau								
M	18°27.8N	21°01.5W	3104	2.205	2.364	0.93	1.42	110.0
K	16°27.2N	21°32.9W	3753	2.209	2.358	0.77	1.17	103.2

The composition of bottom waters was determined for the eastern equatorial Atlantic sites: in situ levels of TCO_2 and A_t; computed Ω_c, saturation index of bottom waters with respect to calcite (Mucci, 1983) and CO_3^{2-}, in situ carbonate ion concentration (after Gehlen et al., 2005).

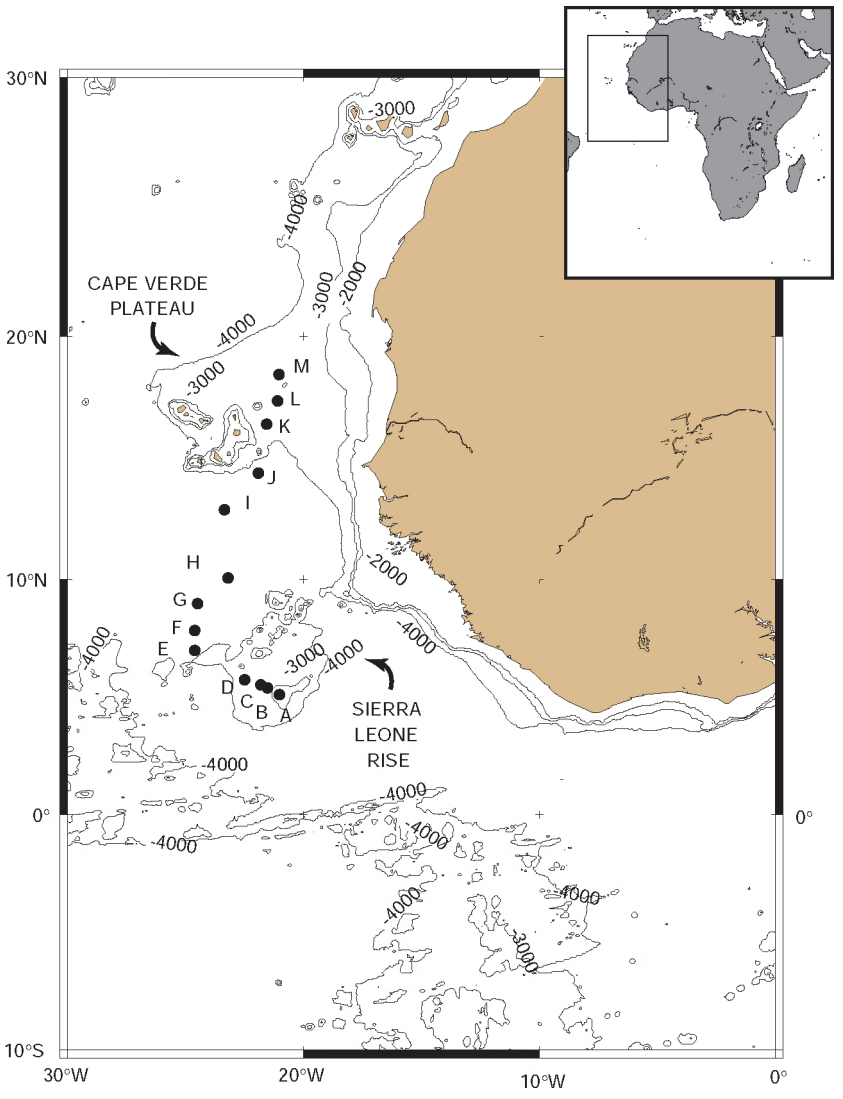

Fig. 1. Location of sampling sites on the Sierra Leone Rise and Cape Verde Plateau.

method (Grasshoff et al., 1983). They were below the detection limit (20 nM/kg). The seawater was brought to the desired initial alkalinity by adding the corresponding volume of a 0.1 M $NaHCO_3$ stock solution. Experiments were run for approximately 50 h in the free-drift mode under constant pCO_2 at 20 °C and with a solid to solution ratio of 1–100. The pCO_2 of the gas mixture ranged between 3100 and 3132 ppm with a manufacturer given precision of 0.3%. At the onset of the experiment, the seawater was equilibrated under constant stirring with a commercial N_2–CO_2 gas mixture until a stable pH was obtained. A known amount of $CaCO_3$ was added to the reactor. The system was closed and stirring was started (glass propeller). The solids were kept in suspension by the combined effect of stirring and bubbling of the gas mixture. The reaction was monitored by following the evolution of solution pH. The speciation of the carbonate system was computed

combining measured pH and known pCO_2. A sample of the experimental solution was withdrawn at the start and at the end of the experiment and analyzed for alkalinity. We combined measured alkalinity (A_t) and known pCO_2 to compute solution pH (Fig. 2) and carbonate alkalinity to check the internal consistency of the carbonate system. If necessary, measured pH values were corrected to correspond to those calculated from A_t and pCO_2 (maximum magnitude of correction of 0.02 pH units). The offset between measured and calculated pH values appeared to be a characteristic of the particular glass electrode. Dissociation constants as recommended by DOE (1994) were used for all calculations. All pH values were reported on the total ion scale (pHt, mol/kg_{sol})

At the end of the experiment, the seawater solution was filtered (0.45 μm) and the solid fraction recovered. The carbonate material was rinsed with distilled water and oven-dried. In order to evaluate the effect of sample heterogeneity, we duplicated experiments for SLR station A and CVP station M. For the duplicated experiments A1, M1, we selected a greater time interval between individual pH measurements. The details of experimental conditions are presented in Table 2.

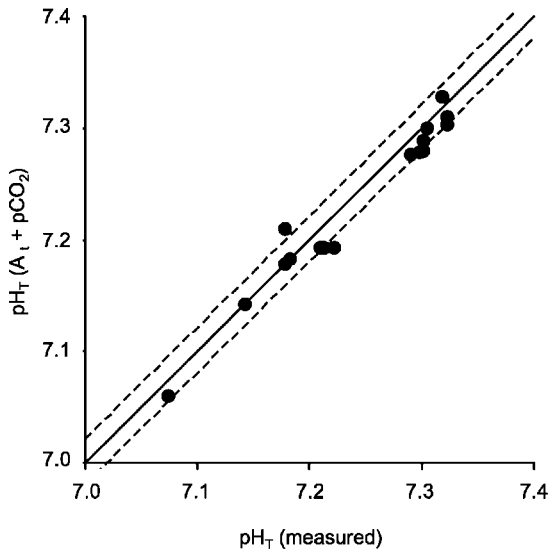

Fig. 2. Comparison between measured and computed solution pH. The computed values were obtained by combining measured alkalinity and pCO_2. Bold line = 1:1 line measured and computed solution pH; dotted line = ±0.02 pH units.

4.2. Analytical procedures

The pH of the experimental seawater (pHt) solution was monitored with a combined glass electrode and a high-precision pH-meter (Radiometer Analytical). The pH electrode was calibrated using two or three NBS buffers combined with a seawater TRIS buffer (Dickson, 1993a, b; Millero et al., 1993). The standard error of pH measurements associated with electrode calibration was below 0.01 pH units (range 0.001–0.01). The stability of pH measurements was checked by monitoring the pH value of a TRIS buffer over a period of 20 h. The electrode was calibrated three times during this interval ($t = 0$, 6, 20 h). The pH value of the TRIS buffer yielded by repeated calibrations fluctuated by ±0.01% (equivalent to 0.8×10^{-3} pH units). Between calibrations, the pH drift over 14 h amounted to 0.6% of its initial value (equivalent to 0.05 pH units). Despite the overall stability of the electrode system, results of several experiments had to be corrected for a linear electrode drift between calibrations. An electrode

Table 2
Details of experimental conditions

Station	Salinity	pCO_2 (ppm)	Ca^{2+} (mmol/kg_{sw})	$A_{t,0}$ (meq/kg_{sw})
Sierra Leone Rise				
A1	33.66	3104	10.61	1.791
A2	33.66	3132	10.13	1.804
C	32.06	3104	9.57	2.008
E	32.06	3100	9.57	2.008
G	32.06	3100	9.57	2.008
Cape Verde Plateau				
M1	33.66	3104	10.13	1.973
M2	32.06	3100	9.57	2.008
K1	32.06	3100	9.57	2.008

Salinity, pCO_2, total alkalinity (meq/kg_{sw}, standard deviation ≤0.01 meq/kg_{sw}). All experiments were run at 20 °C, 1 atm pressure, using artificial seawater.

failure occurred during the dissolution experiments M2 and G. The results could be exploited nevertheless since the pH and the solution composition from speciation (A_t and pCO_2) at 48 h were consistent.

The chlorinity and total alkalinity (A_t) of filtered (0.45 mm millipore filters) solution sub-samples were determined by potentiometric titration. For the chlorinity analysis, the artificial seawater was titrated with $AgNO_3$. The total alkalinity was analyzed following Gieskes and Rogers (1973) by titrating a sub-sample with standardized, commercial dilute HCl 0.01 ($\pm 0.2 \times 10^{-4}$) N. The seawater calcium concentration was determined according to Tsunogai et al. (1968) on randomly selected samples. In order to control the mass balance, the calcium production during dissolution as derived from measurements was compared to the one computed from alkalinity change. The two approaches yielded consistent results. For each titration five replicates were analyzed resulting in a standard error of mean better than 0.2% (range: 0.1–0.2%).

4.3. Data treatment

The time-dependent evolution of pH was converted to carbonate alkalinity (A_c, meq/kg_{sw}) by combining pHt and pCO_2. Dissolution time series were quantified by fitting an empirical relationship to the time-dependent evolution of carbonate alkalinity (A_c, meq/kg_{sw}):

$$A_c(t) = (A_{c,0} - A_{c,\infty}) \exp(-\alpha t^{\beta}) + A_{c,\infty} \quad (1)$$

with

$$A_{c,t} = A_{c,0}, \text{ for } t = 0 \text{ and } A_{c,t} = A_{c,\infty} \text{ for } t \to \infty.$$

The alkalinity $A_{c,\infty}$ corresponds to the alkalinity extrapolated to infinite time ($dA_c/dt = 0$) and is thus an estimate of the apparent solubility of the carbonate sample. We refer to it as asymptotic alkalinity. The asymptotic alkalinity, α and β are free parameters. They were adjusted by minimizing the sum of least squares. The rate of alkalinity production follows from dA_c/dt.

The asymptotic concentration product was derived from the speciation of the carbonate system computed by combining estimated $A_{c,\infty}$ and known pCO_2. It is defined by

$$[Ca^{2+}]_{\infty} \times [CO_3^{2-}]_{\infty} \quad (2)$$

with $[Ca^{2+}]_{\infty} \times [CO_3^{2-}]_{\infty}$, asymptotic concentration product for $t \to \infty$.

The concentration of $[Ca^{2+}]_{\infty}$ was estimated from the total alkalinity production $\Delta A_t = A_{t,\infty} - A_{t,0}$, as $[Ca^{2+}]_{\infty} = [Ca^{2+}]_0 + 0.5 \times \Delta A_t$.

The carbonate dissolution rate is then

$$R = \frac{dA_C}{dt} = k(1 - \Omega)^n \quad (3)$$

with R the dissolution rate (meq/kg_{sw}/time); k the dissolution rate constant (meq/kg_{sw}/time); n the dimensionless order of reaction and Ω the ratio asymptotic over stoichiometric concentration product.

The dissolution rate constant, R, was normalized with respect to the specific surface area of carbonate samples (m^2/kg_{solid}) and the solid to solution ratio (kg_{solid}/kg_{sw}) to yield R_s, the specific rate of dissolution in meq/m^2/time. Reaction order, n, and specific dissolution rate constant, k_s (meq/m^2/time), were estimated by linear regression analysis from the logarithmic form of Eq. (3) after normalization with respect to the specific surface area and the solid to solution ratio

$$\log R_s = n \log(1 - \Omega) + \log k_s \quad (4)$$

with R_s the normalized dissolution rate (meq/m^2/time); k_s the specific dissolution rate constant (meq/m^2/time) and n the dimensionless order of reaction.

5. Results

Total alkalinities of samples taken at the end of dissolution experiments are given in Table 3. The measurement corresponding to experiment M1 (final) is not reported. The measured A_t of the sample taken at the end of this experiment was 2.00 meq/kg_{sw} ($t = 51$ h), which corresponds to a pHt of 7.19 calculated from A_t and pCO_2. The comparison with the measured pHt (7.34) reveals a lack of consistency. The low value of A_t is

Table 3
Dissolution experiments

Station	$A_{t,f}$ (meq/kg$_{sw}$)	$A_{c,\infty}$ (meq/kg$_{sw}$)	$[Ca^{2+}]_\infty \times [CO_3^{2-}]_\infty$ mol/kg$_{sw}$)^2	$\Delta CaCO_3$ (%)	Time (h)
Sierra Leone Rise					
A1	2.789	2.95	6.77×10^{-7}	0.50	50
A2	2.699	3.00	6.56×10^{-7}	0.37	49
C	2.488	2.55	4.37×10^{-7}	0.26	49
E	2.444	2.52	4.27×10^{-7}	0.30	49
G	2.456	2.54	4.34×10^{-7}	0.24	49
Cape Verde Plateau					
M1	n.d.	3.00	6.77×10^{-7}	0.46	51
M2	2.586	2.85	5.50×10^{-7}	0.30	48
K1	2.517	2.55	4.37×10^{-7}	0.27	46

$A_{t,f}$, total alkalinity (meq/kg$_{sw}$, standard deviation $\leqslant 0.01$ meq/kg$_{sw}$) measured at end of times series; $A_{c,\infty}$, asymptotic carbonate alkalinity; $[Ca^{2+}]_\infty \times [CO_3^{2-}]_\infty$, concentration product computed for the asymptotic solution composition; $\Delta CaCO_3$, mass loss during dissolution experiment (% of initial solid mass); time (h), duration of experiment The total alkalinity for experiment M1 is not reported (see text for further details).

attributed to a dilution of the sample, possibly with distilled water during its processing.

The evolution of the solution pH (pHt) as a function of time during dissolution experiments is presented in Fig. 3. During experiments SLRA1, SLRA2, CVPM1 observations were recorded manually; later on the pH-meter was interfaced with a personal computer. Periods without data on curve SLRA2 correspond to time intervals without observations. After calibration, the signal recorded by the pH electrode needed ± 15 min in order to return to its pre-calibration value, resulting in small spikes on the pH curve. The overall shape of the time-dependent evolution of pH is similar among stations. The rapid increase during the first 10 h is followed by the slower evolution thereafter. The curves tend towards a plateau with increasing time. The pH time series recorded for sediments of SLR station A stands out among the experiments with a high final pH of 7.33 reached after 49 h of dissolution. The remaining stations level off at a lower pH values. There is no clear trend with depth.

Fig. 4 exemplifies the time dependent evolution of A_c for SLR stations A, C and CVP stations M and K. The shape of the evolution of carbonate alkalinity (A_c) as a function of time is identical to the one discussed for pH. An electrode failure occurred during experiment CVPK, which explains the lack of data in the second part of the curve. The plain lines are computed following Eq. (1). There is an overall good agreement between computed time series of A_c and the data.

The order of reaction and the specific rate constant of dissolution are derived from linear regression of the double logarithmic plot according to Eq. (4) (Fig. 5). During the 60 min following the introduction of solids a fast increase in pH is observed. It translates into a slight non-linearity of double logarithmic plots during the initial part of the curves. This rapid change in solution chemistry most likely reflects the combined effects of wetting of dry solid surfaces and dissolution of fines adhering to the carbonate particles. It is excluded from linear regression analysis. The reaction order (n) and the specific rate constant of dissolution (k_s) are computed from linear regression to Eq. (4). Results are summarized in Table 4 together with the associated errors.

6. Discussion

6.1. Dissolution time series

The final A_t reached at the end of dissolution experiments (Table 3) might not represent an equilibrium between the solid and the dissolved

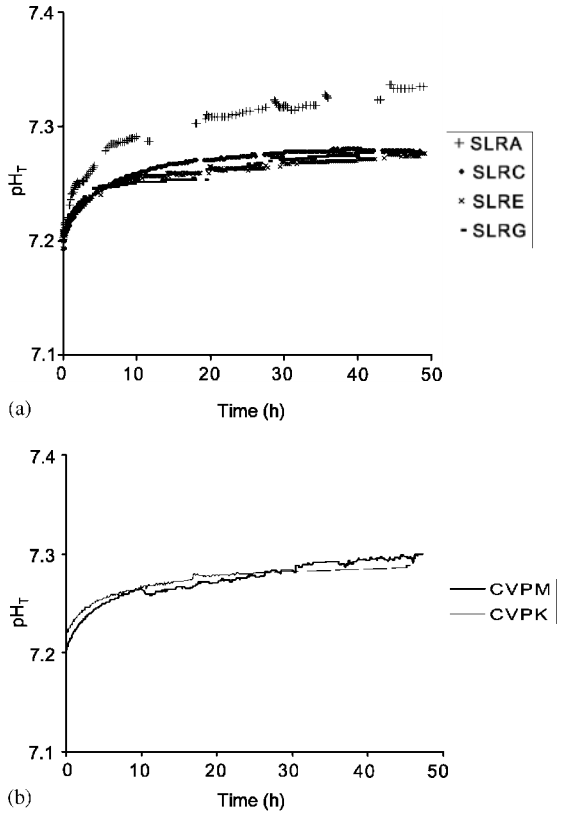

Fig. 3. The evolution of the solution pH as a function of time during dissolution experiments. (a) Sierra Leone Rise bathymetric transect: stations A (SLRA, 2637 m), C (SLRC, 3593 m), E (SLRE, 4202 m), G (SLRG, 4930 m); (b) Cape Verde Plateau bathymetric transect: stations M (CVPM, 3104 m) and K (CVPK, 3753 m).

phase, so we use the asymptotic alkalinity, $A_{c,\infty}$, to estimate the apparent solubility. The corresponding asymptotic concentration product ($[Ca^{2+}]_\infty \times [CO_3^{2-}]_\infty$) is derived from the speciation of the carbonate system computed by combining $A_{c,\infty}$ and pCO_2 (Table 3). Independent solubility estimates were obtained from long-term equilibration experiments using samples from the SLR and the CVP transects (Gehlen et al., 2005). We computed an average stoichiometric concentration product for calcite of 4.37 (± 0.22) $\times 10^{-7}$ mol^2/kg$^2_{sw}$ from 13 independent experiments. Applying the ratio between K^*_{sp}(arag)/K^*_{sp}(calc) of 1.5 (Mucci, 1983) gives a stoichiometric concentration product of aragonite equal to 6.56×10^{-7} mol^2/kg$^2_{sw}$. With the exception of the shallow stations A and M, asymptotic concentration products computed for SLR and Cape Verde samples correspond to the stoichiometric concentration product of calcite. Calcite appears to be the main dissolving phase in these samples.

The asymptotic concentration products for the shallow stations A and M are close to K^*_{sp}(arag). This stands in contrast to the results from long-term equilibration experiments starting from undersaturation with respect to calcite. The independent experiments yielded stoichiometric solubility products for both stations that were not significantly different from those obtained for the deeper sites. They corresponded to calcite solubility. The asymptotic concentration products close to K^*_{sp}(arag) obtained during the short-term kinetic experiments suggest the presence of trace levels of a higher solubility carbonate phase such as aragonite or Mg-calcite. This carbonate phase appears to dominate short-term dissolution experiments. During long-term equilibration experiments, it was fully dissolved before calcite solubility was reached.

The presence of aragonite appears to be the most likely explanation. We did not, however, detect aragonite by X-ray diffraction analysis (Gehlen et al., 2005). The detection limit of XRD for aragonite is ≈ 1 weight %. The maximal mass loss during dissolution experiments of station A was 0.5%, thus below the detection limit (Table 3), and minor admixtures of aragonite cannot be ruled out. Alternatively, the asymptotic concentration products might indicate the presence of a higher solubility carbonate precipitate. Decompression during core retrieval is known to cause carbonate precipitation out of pore waters (Murray et al., 1980). Asymptotic alkalinities would thus reflect the dissolution of this precipitated phase. Pore water DIC data (Martin et al., 2002) suggest that decompression-driven carbonate precipitation could account for at most 0.01% of the bulk $CaCO_3$ content, far below the mass loss during dissolution experiments. Moreover this process would affect all samples and not be restricted to shallow stations.

The asymptotic solubility values for stations A and M could be due to the dissolution of

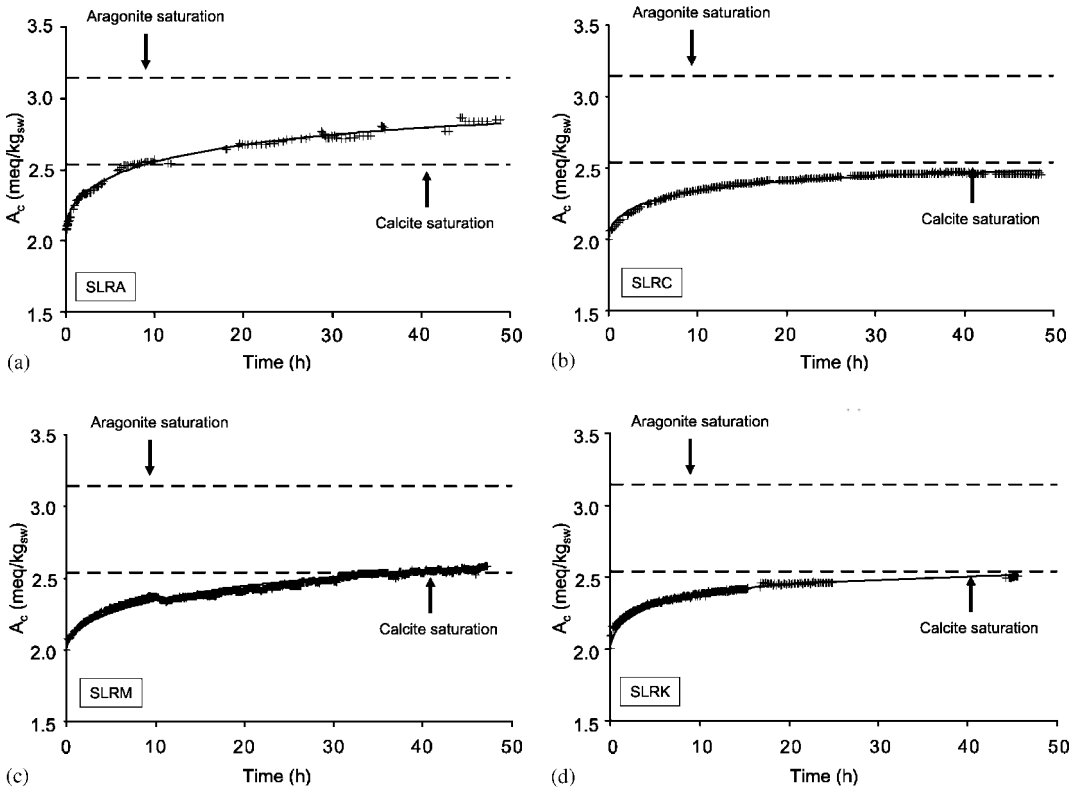

Fig. 4. The evolution of the carbonate alkalinity as a function of time during dissolution experiments. (a) Sierra Leone Rise bathymetric transect: stations A (SLRA, 2637 m) and C (SLRC, 3593 m); (b) Cape Verde Plateau bathymetric transect: stations M (CVPM, 3104 m) and K (CVPK, 3753 m). Carbonate alkalinities corresponding to saturation with respect to calcite and aragonite (Gehlen et al., 2005) are indicated for comparison. Symbols = data; plain line = computed following Eq. (1).

authigenic carbonate phases that precipitated in surface sediments in contact with supersaturated bottom waters. The rapid formation of a Mg-rich carbonate phase and its subsequent recrystallization was documented during long-term equilibration experiments (Gehlen et al., 2005). The saturation index with respect to calcite (Table 1) ranges from 1.62 (station A) to 1.43 (station M). If precipitation occurred at shallow stations A and M despite the known inhibitory effect of phosphate and DOC, we would expect the formation of an inorganic carbonate phase (coating) which would be in equilibrium with the bottom water composition. These abiotic carbonates are likely to have an average Mg content between 8 and 10 mol% (Mucci and Morse, 1990). According to Berner (1976), a magnesian calcite of 8.5 mol% $MgCO_3$ has a solubility close to that of aragonite, which is consistent with the high asymptotic concentration products of stations A and M.

Jahnke and Jahnke (2004) present a review of benthic fluxes of O_2, A_t, Ca^{2+} and nutrients. The CVP station M is part of their study. Comparing sites from a variety of geographic regions, the authors found that at locations with high carbonate sediments and overlain by supersaturated bottom waters, A_t fluxes are greatly depressed compared to those expected from the remineralization rate (metabolic dissolution). At station M, a total of 4 chamber deployments yielded close to zero fluxes of A_t and Ca^{2+}, despite substantial inputs of organic C from the nearby Mauritania upwelling. A possible explanation calls for the inorganic precipitation of $CaCO_3$ at the

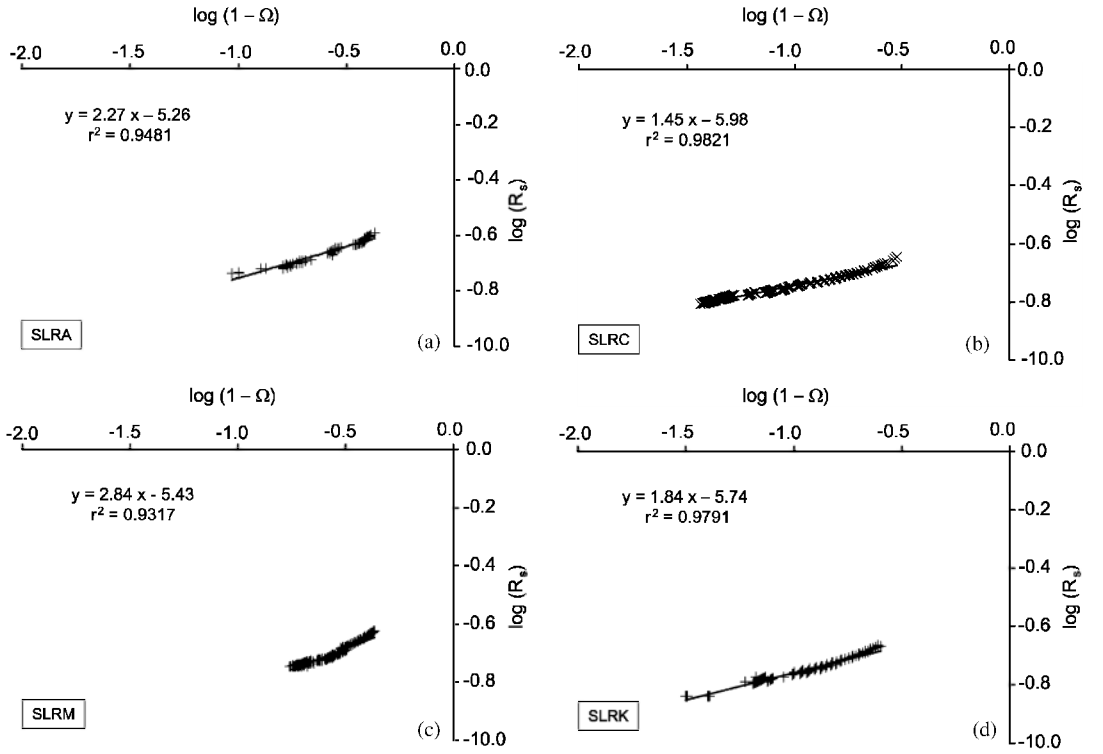

Fig. 5. Examples of double logarithmic plots of the normalized dissolution rate R_s versus $(1-\Omega)$. (a) Sierra Leone Rise bathymetric transect: stations A (SLRA, 2637 m) and C (SLRC, 3593 m); (b) Cape Verde Plateau bathymetric transect: stations M (CVPM, 3104 m) and K (CVPK, 3753 m).

Table 4
Dissolution experiments: reaction order, n and $\log(k_s)$ derived from linear regression along with the associated errors; specific rate constant, k_s

Station	n	Error	$\log(k_s)$	Error	k_s (meq/m^2/d)
Sierra Leone Rise					
A1	2.3	0.11	−5.2519	0.0519	0.48
A2	2.3	0.06	−5.2595	0.0374	0.48
C	1.4	0.01	−5.9833	0.0142	0.09
E	2.3	0.02	−5.2105	0.0132	0.53
G	2.2	0.01	−5.7723	0.0134	0.15
Cape Verde Plateau					
M1	2.6	0.11	−5.4138	0.0636	0.33
M2	2.8	0.03	−5.4266	0.0197	0.32
K1	1.8	0.02	−5.7399	0.0170	0.16

sediment–water interface in contact with supersaturated bottom waters (Jahnke and Jahnke, 2004). Running a diagenetic model with reasonable transport and reaction rates, these authors demonstrated that inorganic precipitation would be a feasible explanation for the benthic flux data. Combining measured O_2 fluxes and associated CO_2 production, we estimated the amount of $CaCO_3$ precipitation needed per year in order to result in zero A_t fluxes at the sediment water interface. Starting out from an average O_2 flux of $(7.8\pm1.6)\times10^{-5}$ mol/cm^3/yr^1 and applying Redfield stoichiometry, Jahnke and Jahnke (2004) calculated an average CO_2 production of $(6.0\pm1.3)\times10^{-5}$ mol/cm^3/yr^1. Part of the CO_2 produced by metabolic activity escapes to the bottom waters without interacting with the carbonate fraction. Assuming a dissolution efficiency of 30% (R. Jahnke, pers. com.), we calculated a metabolic dissolution flux of 1.8×10^{-5} mol C/cm^3/yr^1. Precipitation is expected to occur in contact with bottom waters and to be concentrated at the sediment–water interface. For the purpose

of our first-order calculation, we assume that the authigenic carbonate is distributed homogeneously over the top cm. It follows that in situ precipitation can account for at most 0.01% of the carbonate content of our sample material. While at the present stage we can not rule out the presence of authigenic carbonate phases, they are not a likely quantitative explanation of asymptotic concentration products determined for stations A and M. The presence of trace levels of aragonite is thus the most probable explanation of our results.

6.2. Reaction order and rate constants

A comparison of the reaction order and specific rate constants estimated from replicates of stations SLRA and CVPM (Table 4) shows the good reproducibility of our experimental results. Despite the heterogeneity of natural sediment samples, experiments using different sub-samples of the same station yield similar estimates of reaction order and specific rate constants. Specific rate constants range from 0.09 to 0.53 meq/m^2/d. We estimated reaction orders varying between 1.4 (SLRC) and 2.8 (CVPM2) for samples from the equatorial Atlantic (average $n = 2.3 \pm 0.4$).

The dissolution of biogenic carbonate has been described previously as a higher-order reaction (e.g. Morse, 1978; Keir, 1980). Based upon a re-evaluation of Keir's (1980) results for reagent-grade calcite, Hales and Emerson (1997b) suggested that calcite dissolution in seawater follows first-order kinetics. They argued that the high reaction order of Keir (1980) could reflect uncertainties in the saturation state of the experimental seawater. At this point of the discussion, it is interesting to recall that the dissolution of a homogeneous solid sample will result in a non-linearity with respect to undersaturation only due to the change in specific surface area during dissolution (Wollast, 1965). The observed order of reaction will further depend on particle geometry and, in the case of a powder, on its granulometric distribution.

Marine carbonate assemblages are multi-phase systems, characterized by heterogeneities at the level of the individual carbonate shell (variability in composition and structure due to ontogenesis), as well as at the level of the particle mixture (different species and different particle history). The well-documented with-depth evolution of assemblages in terms of species composition, reflects the heterogeneity at the level of the carbonate particle mixture (Berger, 1970; Berger and Killingley, 1977; Bonneau et al., 1980; Berger et al., 1982). Similarly, the evolution with depth of trace element composition as a result of differential dissolution reflects the heterogeneity at the level of the individual particle (Rosenthal and Boyle, 1993; Lohmann, 1995; McCorkle et al., 1995; Bassinot et al., 2004).

At shallow depths, the presence of aragonite results in two end-members with different rate constants of dissolution and different solubilities. As aragonite disappears from the assemblage by dissolution, we are left with an assemblage made of calcite shells. While the assemblage is now described by a single solubility, different fractions may still be characterized by different specific rate constants. This possibility cannot be directly tested by our kinetic experiments, since we measure a 'bulk' dissolution rate. However, the evolution with depth of physico-chemical parameters provides compelling indirect evidence in support of a range of dissolution rate constants. This evidence includes depth-linked changes of the calcite crystallinity of the size fraction (Gehlen et al., 2005), size-normalized shell weights (Bassinot et al., 2004) and the Mg/Ca of *Globigerinoides ruber* (Beck et al., 2002), which are all consistent with the existence of calcite phases with distinct properties and their differential loss during dissolution.

A simple thought experiment shows how experimental determinations of dissolution reaction order will be influenced by the existence of phases with identical solubilities but different dissolution rate constants. Consider a two-phase system with a single solubility, in which phase A has a faster specific reaction rate than phase B, but is less abundant. During the initial part of the experiment, the total reaction will be dominated by dissolution of phase A. The observer will record a linear ($n = 1$) dependence on solution composition. If the duration of the experiment is sufficiently long, phase A will vanish and the reaction will be dominated by dissolution of phase B. The

overall reaction will slow down and the reaction will no longer be linear with respect to $(1-\Omega)$. For the observer, this behavior is now described by a higher-order reaction ($n=2$). The shifting relative contribution of concomitantly occurring reactions will thus determine reaction order and specific rate constants of individual experiments, and in general, a higher-order reaction is expected to result from such a multi-phase system (Ho and Aris, 1987).

Keir (1980) presents dissolution rate data for synthetic calcite and aragonite, and for the corresponding biogenic phases (monospecific foraminiferal samples and mixed pteropods) and sediment fractions (granulometric size classes). Keir used a stirred-flow reactor under steady-state conditions (chemostat) while we used the free-drift approach described above. Keir's experiments were run at atmospheric pressure and 20 °C in artificial seawater, as were our experiments. He determined the reaction order of calcite dissolution from experiments with synthetic calcite. The resulting estimate of $n(=4.5)$ was used by Keir to evaluate results obtained for biogenic and sedimentary material. Keir's original results are reproduced in Table 5a. We first used Keir's original data on undersaturation $(1-\Omega_c)$ and the dissolution rate normalized to the specific surface area of the sample to derive n and the specific rate constant of dissolution by linear regression of these data to Eq. (4) (Table 5b). In a second approach, we recalculated $(1-\Omega_c)$ from the solution composition given by Keir (1980) and the stoichiometric concentration product of calcite, K^*_{sp}(calc) from our dissolution experiments Gehlen et al. (2005) (Table 5c).

The reaction rate order and specific rate constant of dissolution was derived as described before. The errors associated with estimates of n and k_s from Keir's data are larger than those from our study. This is probably due to the differences in experimental approaches. During a free-drift experiment a large amount of data are recorded over a range of undersaturation. In contrast, the chemostat approach allows for the direct determination of the rate corresponding to a given solution composition. Approach 1 (Keir's data, our estimation procedure, Table 5b) yields values of n ranging from 3.2 to 4.9. Given the uncertainty associated with these estimates, setting $n=4.5$ (Keir, 1980) is acceptable. We note that the parameters n and k_s are not independent. For a given rate of dissolution, changing n will result in a corresponding change in k_s. This explains the differences in k_s estimates (Table 5b) compared to values published by Keir (1980).

The interpretation of results of the dissolution experiments in terms of the dependence on $(1-\Omega_c)$ is very sensitive to uncertainties in the saturation state of the solution. Accordingly, Hales and Emerson (1997b) suggest an overestimation of the stoichiometric solubility product of calcite by Keir to be at the origin of the high reaction order. Uncertainties in $(1-\Omega_c)$ originate either from the choice of carbonic acid dissociation constants selected for the calculation of the speciation of the carbonate system or from the

Table 5
Re-evaluation of data by Keir (1980)

Station	n	Error	Log(k_s)	Error	k_s (meq/m^2/d)
(a) Keir (1980), original data					
G. sacculifer	4.5				1.81
G. bulloides	4.5				5.26
G. pachyderma	4.5				10.3
Rio Grande Rise	4.5				64.7
(b) Ω_c after Keir (1980)					
G. sacculifer	4.0	1.10	0.1126	0.3497	1.30
G. bulloides	3.2	0.65	0.2446	0.2629	1.76
G. pachyderma	4.3	0.73	0.9298	0.2717	8.51
Rio Grande Rise	4.9	0.90	1.9581	0.4194	90.8
(c) Ω_c after Gehlen et al., 2005					
G. sacculifer	3.3	0.90	0.0379	0.3272	1.09
G. bulloides	2.5	0.52	0.1124	0.2471	1.30
G. pachyderma	3.4	0.58	0.7948	0.2535	6.23
Rio Grande Rise	3.6	0.70	1.6962	0.3874	49.7

First set, *original data*, specific rate constant as given by Keir assuming $n=4.5$; second set, *Ω after Keir*, n and k_s estimated from Keir's original data using his stoichiometric concentration product; *Ω after Gehlen* et al., n and k_s estimated from Keir's original data but with the calcite stoichiometric concentration product by Gehlen et al., 2005.
Monospecific foraminifera samples of *Globigerinoides sacculifer*, *Globigerinoides bulloides*, *Globoquadrina pachyderma*; Rio-Grande Rise = 125–250 μm sediment fraction.

selection of the stoichiometric solubility product of calcite K^*_{sp}(calc). Both are discussed in detail by Gehlen et al. (2005). The need for homogeneity in experimental conditions (e.g. natural versus artificial seawater) when selecting dissociation constants and stoichiometric solubility products leads us to select K^*_{sp}(calc) reported in Gehlen et al. (2005). This K^*_{sp}(calc) value is 9% lower than the mean of Keir's estimates. As a result of the lower K^*_{sp}(calc), the recalculated values of n range between 2.5 ± 0.5 and 3.6 ± 0.7 (Table 5c). The comparison between Tables 5b and c provides an estimate of the sensitivity of the calculation to K^*_{sp}. While the new estimates of n are lower than the original ones, they are still greater than unity. Due to the limited number of data available for each sample and their scatter, the reaction order cannot be determined with great confidence.

The revised k_s (Table 5c) are also lower than Keir's original estimates (Table 5b). They are compared to estimates from this study in Fig. 6. While the rate constants estimated for *G. sacculifer* and *G. bulloides* are roughly 4 times higher than those estimated for SLR and CVP samples, an exceptionally high estimate was obtained for *G. pachyderma*. The uncertainty associated with foraminifer data is, however, large and the results have to be viewed with caution. Since n and k_s cannot be estimated with great confidence from Keir's data, we decided to calculate the specific reaction rate R_s at $\Omega_c = 0.8$. The resulting specific reaction rates of Keir's foraminifer samples and our data set are compared in Fig. 7. Error bars are included to show the effect of combined uncertainties on n and k_s. The range limited by the error bars is not centred on the rate estimate because of the non-linear reaction kinetics. Values of R_s up to 5.1 meq/m^2/yr were determined for the SLR transect. The rate calculated for Keir's Rio Grande Rise sample is excluded from the figure. It equals 53 meq/m^2/yr and has an associated uncertainty range between 7.0 and 402 meq/m^2/yr. Our new rates are comparable to the estimate of *G. sacculifer*. They are lower than those of *G. bulloides* and *G. pachyderma*, but fall within the range of uncertainty associated with these results. While the uncertainty associated with the older data limits the comparison between results, it highlights the need of additional experimental work. Clearly, the puzzle of marine carbonate dissolution behaviour can be resolved only through carefully controlled experimental investigation.

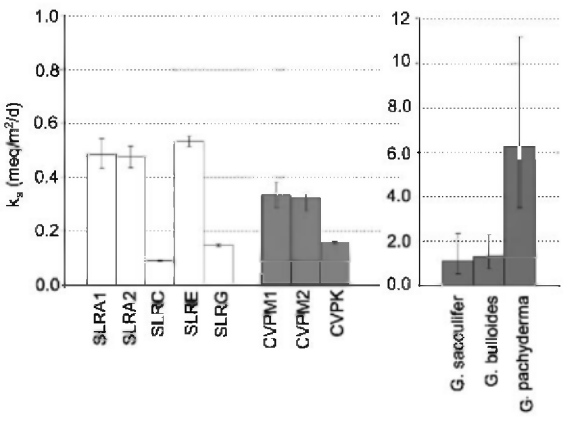

Fig. 6. Comparison of specific dissolution rate constants determined during this study and re-evaluated estimates by Keir (1980). Error bars correspond to the error associated with the linear regression used to estimate k_s. Note the different scales of Y-axis.

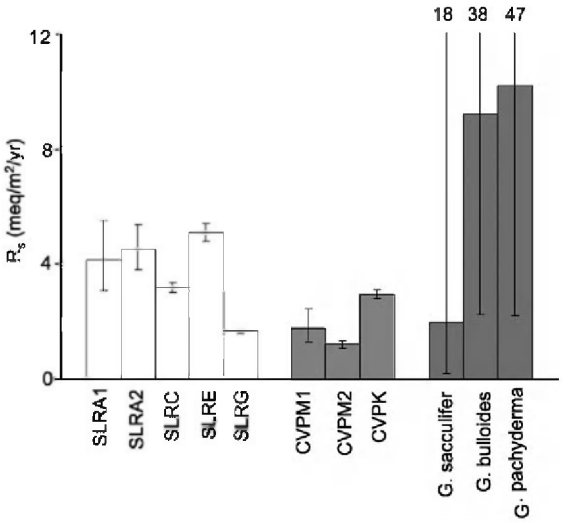

Fig. 7. Specific rate constants computed for $\Omega = 0.8$. Results from this study are compared to estimates by Keir (1980). Error bars indicate the cumulative error associated with estimates of n and k_s.

7. Conclusion

We studied the dissolution kinetics of the greater than 150 μm size fraction of sediments from the eastern tropical Atlantic samples along two bathymetric transects: the Sierra Leone Rise and the Cape Verde Plateau. The asymptotic alkalinity derived from free drift experiments carried out for approximately 50 h at constant pCO_2 ($\approx$3100 ppm) suggests the presence of trace amounts of a higher solubility phase in sediments of the shallow stations (SLRA, 2637 m; CVPM, 3104 m). While it is likely that this phase is aragonite, the presence of authigenic carbonate precipitated in contact with supersaturated bottom waters cannot be excluded. Calcite is the main dissolving phase in sediments from the other stations. The asymptotic concentration products derived from free drift experiments are compatible with the stoichiometric concentration product of aragonite (6.56×10^{-7} mol^2/kg$^2_{sw}$) and calcite ($4.37\ (\pm 0.22) \times 10^{-7}$ mol^2/kg$^2_{sw}$) derived during long-term equilibration experiments.

The order of reaction derived from dissolution time series was always greater than unity. It varies between 1.4 (SLRC) and 2.8 (CVPM2), with an average $n = 2.3 \pm 0.4$. The higher reaction order is explained in terms of a multiphase system. It results from the concomitant dissolution of carbonate fraction characterized by variable reaction rate constant.

Specific rate constants range from 0.09 to 0.53 meq/m^2/d. Estimates of k_s obtained for replicate experiments of stations SRLA and CVPM show no within station variability, which suggests that differences between stations are significant.

The combination of independent long-term equilibration experiments and kinetic experiments carried out on the same material provides a new and improved picture of the dissolution of marine carbonates.

Acknowledgements

M.G. acknowledges the hospitality received during the cruise KN159. Special thanks to the crew of R.V. *Knorr* and all the cruise participants for their help and support. B. Thièbaut helped with the experimental work. We thank B. Hales for insightful comments and generous discussions with M.G. and D.M. We acknowledge the beneficial reviews by R. Jahnke and R. Keir. This study benefited from funding to M.G. by the French national science program INSU/PROOF and the EC (ORFOIS EVK2-CT-2001-00100). The support to LC from the Belgian Federal Office for Scientific, Technical and Cultural Affairs (Contract no. EV/11/5A) and the awards to DMC from the US National Science Foundation (OCE-9730932 and OCE0083314) are also acknowledged. This is LSCE contribution 1342.

References

Arakaki, T., Mucci, A., 1995. A continuous and mechanistic representation of calcite reaction-controlled kinetics in dilute solutions at 25 °C and 1 atm total pressure. Aquatic Geochemistry 1, 105–130.

Archer, D., Maier-Reimer, E., 1994. Effect of deep-sea sedimentary calcite preservation on atmospheric CO_2 concentration. Nature 367, 260–263.

Archer, D., Kheshgi, H., Maier-Reimer, E., 1998. Dynamics of fossil fuel CO_2 neutralization by marine $CaCO_3$. Global Biogeochemical Cycles 12 (2), 259–276.

Archer, D., Emerson, S., Smith, C.R., 1989. Dissolution of calcite in deep-sea sediments: pH and O2 microelectrode results. Geochimica et Cosmochimica Acta 53, 2831–2845.

Archer, D., Winguth, A., Lea, D., Mahowald, N., 2000. What caused the glacial/interglacial atmospheric *p*CO2 cycles? Reviews of Geophysics 38, 159–189.

Bassinot, F.C., Mélières, F., Gehlen, M., Levi, C., Labeyrie, L., 2004. Crystallinity of foraminifer shells: a proxy to reconstruct past CO32-changes? Geochemistry, Geophysics, Geosystems 5, Q08D10.

Beck, L., Bassinot, F., Gehlen, M., Trouslard, Ph., Pellegrino, S., Levi, C., 2002. Detection limit improvement for Mg in marine foraminiferal calcite by using helium induced X-ray emission. Nuclear Instruments and Methods in Physics Research B 190, 482–487.

Berelson, W.M., Hammond, D.E., Cutter, G.A., 1990. In situ measurements of calcium carbonate dissolution rates in deep-sea sediments. Geochimica et Cosmochimica Acta 54, 3013–3020.

Berger, W.H., 1970. Planktonic foraminfera: selective solution and the lysocline. Marine Geology 8, 111–138.

Berger, W.H., Killingley, J.S., 1977. Glacial–Holocene transition in deep-sea carbonates: selective dissolution and the stable isotope signal. Science 197, 563–566.

Berger, W.H., Bonneau, M.-C., Parker, F.L., 1982. Foraminifera on the deep-sea floor: lysocline and dissolution rate. Oceanologica Acta 5 (2), 249–258.

Berger, W.H., Smetacek, V.S., Wefer, G., 1989. Ocean productivity and paleoproductivity—an overview. In: Berger, W.H., Smetacek, V.S., Wefer, G. (Eds.), Productivity of the Ocean: Present and Past. Wiley, New York, pp. 1–34.

Berner, R.A., 1976. The solubility of calcite and aragonite in seawater at atmospheric pressure and 34.5‰ salinity. American Journal of Science 276, 713–730.

Berner, R.A., Morse, J.W., 1974. Dissolution kinetics of calcium carbonate in seawater. IV. Theory of calcite dissolution. American Journal of Science 274, 108–134.

Bonneau, M.-C., Vergnaud-Grazzini, C., Berger, W.H., 1980. Stable isotope fractionation and differential dissolution in recent planktonic foraminifera from Pacific box cores. Oceanologica Acta 3 (3), 377–382.

Broecker, W.S., Takahashi, T., 1978. The relationship between lysocline dpeth and in situ carbonate ion concentration. Deep-Sea Research 25, 65–95.

Broecker, W.S., Klas, M., Clark, E., Bonani, G., Ivy, S., Wolfli, W., 1991. The influence of $CaCO_3$ dissolution on core top radiocarbon ages for deep-sea sediments. Paleoceanography 6, 593–603.

Cai, W.-J., Reimers, C.E., Shaw, T., 1995. Microelectrode studies of organic carbon degradation and calcite dissolution at a California continental rise site. Geochimica et Cosmochimica Acta 59, 497–511.

Chou, L., Garrels, R.M., Wollast, R., 1989. A comparative study of the kinetics and mechanisms of dissolution of carbonate minerals. Chemical Geology 78, 269–282.

Curry, W.B., Lohmann, G.P., 1985. Carbon deposition rates and deep water residence time in the equatorial Atlantic Ocean through-out the last 160,000 years. In: Sundquist, E.T., Broecker, W.S. (Eds.), The Carbon Cycle and Atmospheric CO_2: Natural Variations, Archean to Present; Geophysical Monograph Series 32, pp. 285–302.

Curry, W.B., Lohmann, G.P., 1986. Late quaternary carbonate sedimentation at the Sierra Leone Rise (Eastern Equatorial Atlantic Ocean). Marine Geology 70, 223–250.

Curry, W.B., Lohman, G.P., 1990. Reconstructing past particle fluxes in the tropical Atlantic Ocean. Paleoceanography 5, 487–505.

Dickson, A.G., 1993a. The measurement of sea water pH. Marine Chemistry 44, 131–142.

Dickson, A.G., 1993b. pH buffers for sea water media based on total hydrogen ion concentration scale. Deep-Sea Research I 40, 107–118.

DOE, 1994. Handbook of methods for the analysis of the various parameters of the carbon dioxide system in sea water (version 2). In: Dickson, A.G., Goyet, C. (Eds.), ORNL/CDIAC-74. Carbon Dioxide Information Analysis Center, Oak Ridge National Laboratory, US Department of Energy, Oak Ridge, TN.

Dubois, L.G., Prell, W.L., 1988. Effects of carbonate dissolution on the radiocarbon age structure of sediment mixed layers. Deep-Sea Research 35, 1875–1885.

Emerson, S., Bender, M.L., 1981. Carbon fluxes at the sediment-water interface of the deep-sea: calcium carbonate preservation. Journal of Marine Research 39, 139–162.

Farrel, J.W., Prell, W.L., 1989. Climate change and $CaCO_3$ preservation: an 800,000 year bathymetric reconstruction from the central equatorial Pacific Ocean. Paleoceanography 4, 447–466.

Gehlen, M., Mucci, A., Boudreau, B., 1999. Modelling the distribution of stable carbon isotopes in porewaters of deep-sea sediments. Geochimica et Cosmochimica Acta 63, 2763–2773.

Gehlen, M., Bassinot, F.C., Chou, L., McCorkle D., 2005. Reassessing the dissolution of marine carbonates. Part I: solubility. Deep-Sea Research I 52, this volume, doi:10.1016/j.dsr.2005.03.010.

Gieskes, J.M., Rogers, W.C., 1973. Alkalinity determination in interstitial waters of marine sediments. Journal of Sedimentary Petrology 34, 272–277.

Grasshoff, K., Ehrhardt, M., Kremling, K., 1983. Methods of Seawater Analysis. Verlag Chemie, Weinheim 419pp.

Hales, B., Emerson, S., 1997a. Calcite dissolution in sediments of the Ceara Rise: in situ measurements of porewater O_2, pH, and $CO_{2(aq)}$. Geochimica et Cosmochimica Acta 61, 504–514.

Hales, B., Emerson, S., 1997b. Evidence in support of first-order dissolution kinetics of calcite in seawater. Earth and Planetary Science Letters 148, 317–327.

Hales, B., Emerson, S., Archer, D., 1994. Respiration and dissolution in the sediments of the western North Atlantic: estimates from models of in situ microelectrode measurements of porewater oxygen and pH. Deep-Sea Research I 41, 695–719.

Ho, T.C., Aris, R., 1987. On apparent second-order kinetics. American Institute of Chemical Engineering Journal 1, 129–135.

Honjo, S., Erez, J., 1978. Dissolution rates of calcium carbonates in the deep ocean: an in-situ experiment in the North Atlantic Ocean. Earth and Planetary Science Letters 40, 287–300.

Ingle, S.E., Culberson, C.H., Hawley, J.B., Pytkowicz, R.M., 1973. The solubility of calcite in sea water at atmospheric pressure and 35‰ salinity. Marine Chemistry 1, 295–307.

Jahnke, R.A., Craven, D.B., McCorkle, D.C., Reimers, C.E., 1997. Ca CO_3 dissolution in California continental margin sediments: the influence of organic matter mineralization. Geochimica et Cosmochimica Acta 61, 3587–3604.

Jahnke, R.A., Jahnke, D.B., 2004. Calcium carbonate dissolution in deep sea sediments: reconciling microelectrode, pore water and benthic flux chamber results. Geochimica et Cosmochimica Acta 68, 47–59.

Keir, R.S., 1980. The dissolution kinetics of biogenic carbonate in seawater. Geochimica et Cosmochimica Acta 44, 241–252.

Lohmann, G.P., 1995. A model for variation in the chemistry of planktonic foraminifera due to secondary calcification and selective dissolution. Paleoceanography 10, 115–457.

Lyle, M., Murray, D.W., Finney, B.P., Dymond, J., Robbins, J.M., Brooksforce, K., 1988. The record of late Pleistocene biogenic sedimentation in the eastern tropical Pacific. Oceanic Paleoceanography 3, 39–59.

Martin, W.R., McNichol, A.P., McCorkle, D.C., 2000. The radiocarbon age of calcite dissolving at the sea floor: estimates from pore water data. Geochimica et Cosmochimica Acta 64, 1391–1404.

Martin, W.R., McCorkle, D.C., McNichol, A.P., Sayles, F.L., 2002. Radiocarbon in pore water carbon pools in sediments of the Eastern Equatorial Atlantic Ocean. Eos Transactions AGU 83, Ocean Science Meeting Supplement OS51I-05 (abstract).

McCorkle, D.C., Martin, P.A., Lea, D.W., Klinkhammer, G.P., 1995. Evidence of a dissolution effect on benthic foraminiferal shell chemistry: $\delta^{13}C$, Cd/Ca, Ba/Ca, and Sr/Ca results from the Ontong Jave Plateau. Paleoceanography 10, 699–714.

Millero, F.J., 1995. Thermodynamics of the carbon dioxide system in the oceans. Geochimica et Cosmochimica Acta 59, 661–677.

Millero, F.J., Zhang, J.-Z., Fiol, S., Sotolongo, S., Roy, R.N., Kitack, L., Mane, S., 1993. The use of buffers to measure the pH of seawater. Marine Chemistry 44, 143–152.

Morse, J.W., 1978. Dissolution kinetics of calcium carbonate in seawater. VI. The near-equilibrium dissolution kinetics of carbonate-rich deep-sea sediments. American Journal of Science 278, 344–353.

Morse, J.W., Berner, R.C., 1972. Dissolution kinetics of calcium carbonate in sea water. II: a kinetic origin for the lysocline. American Journal of Science 272, 840–851.

Morse, J.W., Arvidson, R.S., 2002. The dissolution kinetics of major sedimentary carbonate minerals. Earth-Science Reviews 58, 51–84.

Mucci, A., 1983. The solubility of calcite and aragonite in seawater at various salinities, temperatures and one atmosphere total pressure. American Journal of Science 283, 780–799.

Mucci, A., Morse, J.W., 1990. Chemistry of low-temperature abiotic calcites: experimental studies on coprecipitation, stability, and fractionation. Review of Aquatic Sciences 3, 217–254.

Murray, J.W., Emerson, S., Jahnke, R., 1980. Carbonate saturation and the effect of pressure on the alkalinity of interstitial waters from the Guatemala Basin. Geochimica et Cosmochimica Acta 44, 963–972.

Opdyke, B.N., Walker, J.C.G., 1992. Return of the coral reef hypothesis: basin to shelf partitioning of $CaCO_3$ and its effect on atmospheric CO_2. Geology 20, 733–736.

Plummer, L.N., Wigley, T.M.L., Parkhurst, D.L., 1978. The kinetics of calcite dissolution in CO_2–water systems at 5–60 °C and 0.0 to 1.0 atm CO_2. American Journal of Science 278, 179–216.

Rosenthal, Y., Boyle, E., 1993. Factors controlling the fluoride content of planktonic foraminifera: an evaluation of its paleoceanographic applicability. Geochimica et Cosmochimica Acta 57, 335–346.

Sigman, D.M., McCorkle, D.C., Martin, W.R., 1998. The calcite lysocline as a constraint on glacial–interglacial low latitude production changes. Global Biogeochemical Cycles 12, 409–427.

Tsunogai, S., Nishimura, M., Nakaya, S., 1968. Complexometric titration of calcium in the presence of larger amounts of magnesium. Talanta 15, 385–390.

Van Cappellen, P.V., Charlet, L., Stumm, W., Wersin, P., 1993. A surface complexation model of the carbonate mineral–solutions interface. Geochimica et Cosmochimica Acta 57, 3503–3518.

Walter, L.M., Morse, J.W., 1985. The dissolution kinetics of shallow marine carbonates in seawater: a laboratory study. Geochimica et Cosmochimica Acta 49, 1503–1514.

Wollast, R., 1965. Influence de quelques facteurs physiques sur la cinétique des réactions l'etat solide. Industrie Chimique Belge 30, 473–479.